

Double Ionization Dynamics of Molecules in an Ultrashort Intense Laser Pulse with Long-Wavelength

J. Liu¹, D.F. Ye^{1,2}, and J. Chen¹

1. Institute of Applied Physics and Computational Mathematics, P.O.Box 100088, Beijing, P. R. China

*2. Graduate School, China Academy of Engineering Physics,
P.O. Box 8009-30, Beijing, 100088, P. R. China*

We develop a semiclassical quasi-static model that quantitatively accounts for experimental data on the double ionization of nitrogen molecules for a wide range of laser intensities from tunnelling regime to over-barrier regime. With this model, we achieve insight into the correlated dynamics of two valence electrons in combined two-center nuclear attraction and intense laser force, and reveal the significant influence of molecular alignment on double ionization yield.

PACS numbers: 33.80.Rv, 34.80.Gs, 42.50.Hz

Experimental data from double ionization (DI) of atoms and molecules by short intense laser pulses are of great interest in strong-field physics because they reveal highly correlated electron-electron behavior[1, 2, 3, 4]. For molecules have more degrees of freedom than atoms, their DI dynamics is expected to be more complicated. Evidence is that recent data exposed the significant influence of molecular structure as well as molecular alignment on both double ionization yield and ionized-electron momentum distributions[5, 6, 7].

Even for simple hydrogen-molecule-like nitrogen molecule, physics behind its double ionization data is far from being settled, and theoretical exploration is extensive. The fully time-dependent dynamics of the pairwise $e-e$ responding to two-center nuclear attraction and laser force poses a daunting challenge for any quantum theoretical treatment[8]. Recent years witness the renaissance of classical treatment because evidence has been accumulating that a purely classical scenario is consistent with many of the observed double-ionization effects[9, 10]. However, purely classical treatment has its unreachable regime of quantum tunnelling, where most current experiments work. Therefore, results from the above purely classical calculations can not be compared with experimental data quantitatively.

In this letter, we provide an alternative way, i.e. semiclassical approach. Our semiclassical quasi-static model is capable to quantitatively account for the DI experimental data of nitrogen molecules for a wide range of laser intensities, i.e., from tunnelling regime to over-barrier regime (see Fig.1). With this model, we reproduce unusual excess DI rate in the range from $5 \times 10^{13} \text{W/cm}^2$ to $1 \times 10^{15} \text{W/cm}^2$, where DI yield could be one million times higher than that calculated from uncorrelated sequential theory. In particular, the significant influence of molecular alignment on DI yield is virtually revealed by our model.

Model.— We consider a molecule of two valence electrons interacting with a laser pulse whose temporal and spatial distribution is expressed as $\varepsilon(t) = \varepsilon_0(R_L, Z_L) \sin^2(\frac{\pi t}{nT}) \cos(\omega t) \mathbf{e}_z$. The external field along the propagation direction of the laser beam is approx-

imately constant and in the lateral direction it can be treated as an ideal Gaussian beam, i.e., $\varepsilon_0(R_L, Z_L) = \varepsilon_0(R_L) = \varepsilon_0 \exp(-R_L^2/R_0^2)$, where ε_0 is the peak laser field, R_L represents the position of the molecules in the laser beam, and R_0 is the radius of the beam. A \sin^2 enveloped laser with the full width of nT is used in our calculations, where T and ω are period and angular frequency of the laser field respectively and n denotes the number of optical cycles.

In the long-wavelength limit, the above laser field varies slowly in time and can be regarded as a quasi-static field compared to valence electron's circular motion around nuclei. Under this field, the Coulomb potential between nuclei and electrons is significantly distorted. When the instantaneous field (at time t_0) is smaller than a threshold value (see Fig.2(a)), one electron is released

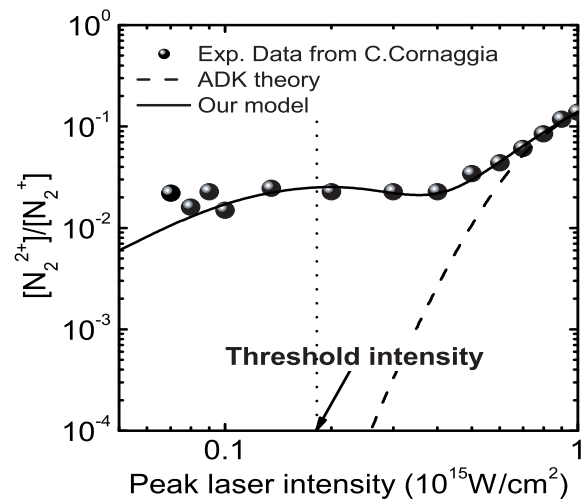


FIG. 1: (color online). Comparison between DI data[3] and theory for nitrogen molecule. 0.185PW/cm^2 is the threshold intensity separates the tunnelling regime and over barrier regime as schematically plotted in Fig.2. To our knowledge, the results from our theoretical model are the first to be in good agreement with experimental data for a wide range of laser intensities from tunnelling regime to over-barrier regime.

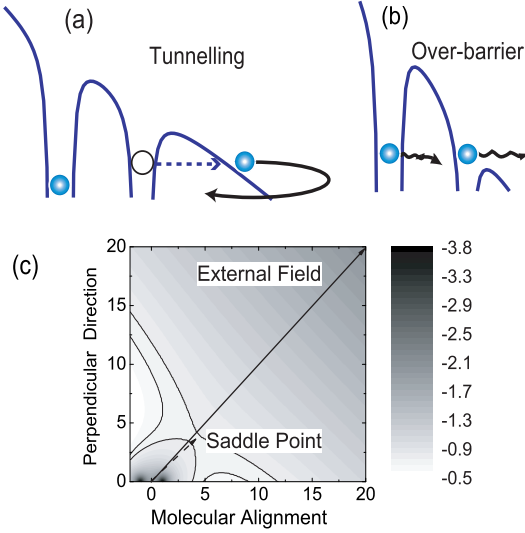


FIG. 2: (color online). (a) Tunnelling ionization. (b) Over-barrier ionization. (c) The contour plot of the combined Coulomb potential and external field. It clearly shows that the saddle point locates approximately along the direction of the external field.

at the outer edge of the suppressed Coulomb potential through quantum tunnelling with a rate $\varpi(t_0)$ given by molecular ADK formula[11].

The electron tunnels out through a saddle point[10] directing to a channel of the local minimum in the combined potential of the Coulomb interaction and the external field (see, Fig.2(c)). Because the difference between the direction of the saddle point and the external field is very small, we safely regard the external field direction (z axis) as the tunnelling direction. Thus, the initial position of the tunnelled electron can be derived from following equation,

$$-\frac{1}{r_{a1}} - \frac{1}{r_{b1}} + \int \frac{|\Psi(\mathbf{r}')|^2}{|\mathbf{r}_1 - \mathbf{r}'|} d\mathbf{r}' + I_{p1} - z_1 \varepsilon(t_0) = 0, \quad (1)$$

with $x_1 = y_1 = 0$. The wavefunction Ψ is given by the linear combination of the atomic orbital-molecular orbital (LCAO-MO) approximation. Taking N_2^+ for example, we choose $\phi(r) = \frac{\lambda^{3/2}}{\sqrt{\pi}} e^{-\lambda r}$ as the trial function to construct the molecular orbital $\Psi(r) = c[\phi(r_{a2}) + \phi(r_{b2})]$, where c is the normalization factor. The parameter λ , which equals to 1.54 for N_2^+ , is determined through variational approach. The initial velocity of tunnelled electron is set to be $(v_{\perp} \cos \varphi, v_{\perp} \sin \varphi, 0)$, with v_{\perp} having the same distribution as that in atomic case, i.e., $w(v_{\perp}) dv_{\perp} = \frac{2(2I_{p1})^{1/2} v_{\perp}}{\varepsilon(t_0)} \exp(-\frac{v_{\perp}^2 (2I_{p1})^{1/2}}{\varepsilon(t_0)}) dv_{\perp}$ where φ is the polar angle of the transverse velocity uniformly distributed in the interval $[0, 2\pi]$. For the bounded electron, the initial position and momentum are depicted by single-electron microcanonical distribution (SMD)[13] $F(\mathbf{r}_2, \mathbf{p}_2) = k\delta[I_{p2} - \mathbf{p}_2^2/2 - W(r_{a2}, r_{b2})]$, where k is the normalization factor,

I_{p2} denotes the ionization energy of molecular ions such as N_2^+ , and $W(r_{a2}, r_{b2}) = -1/r_{a2} - 1/r_{b2}$ is the total interaction potential between the bound electron and two nuclei.

The above scheme is a direct extension of our quasi-static model for atomic DI[14] and is available only when instantaneous field is below the threshold value. To give a complete description of the DI of molecular system for the whole range of the laser intensities (see Fig.1), it is required to further extend our model to the over-barrier regime (Fig.2b). This is done by constructing initial conditions with double-electron microcanonical distribution (DMD)[15], i.e., $F(\mathbf{r}_1, \mathbf{r}_2, \mathbf{p}_1, \mathbf{p}_2) = \frac{1}{2}[f_{\alpha}(\mathbf{r}_1, \mathbf{p}_1)f_{\beta}(\mathbf{r}_2, \mathbf{p}_2) + f_{\beta}(\mathbf{r}_1, \mathbf{p}_1)f_{\alpha}(\mathbf{r}_2, \mathbf{p}_2)]$, with $f_{\alpha, \beta}(\mathbf{r}, \mathbf{p}) = k\delta[I_{p1} - \frac{\mathbf{p}^2}{2} - W(r_a, r_b) - V_{\alpha, \beta}(\mathbf{r})]$, where $V_{\alpha, \beta}(\mathbf{r})$ represents mean interaction between the electrons, $V_{\alpha, \beta}(\mathbf{r}) = \frac{1}{r_{b, \alpha}}[1 - (1 + \kappa r_{b, \alpha})e^{-2\kappa r_{b, \alpha}}]$. κ can be obtained by a variational calculation of the ionization energy of molecules (1.14 for N_2).

The subsequent evolution of electron pairwise with the above initial conditions is simulated by classical Newtonian equations:

$$\frac{d^2 \mathbf{r}_i}{dt^2} = \varepsilon(t) - \nabla(V_{ne}^i + V_{ee}). \quad (2)$$

Here index i denotes the two different electrons. V_{ne}^i and V_{ee} are Coulomb interaction between nuclei and electrons and between two electrons, respectively, $V_{ne}^i = -\frac{1}{r_{ai}} - \frac{1}{r_{bi}}$, $V_{ee} = \frac{1}{|\mathbf{r}_1 - \mathbf{r}_2|}$, where r_{ai} and r_{bi} are distances between the i th electron and nucleus a and b , respectively. The above Newtonian equations is solved using the 4-5th Runge-Kutta algorithm and DI events are identified by energy criterion. In our calculations, more than 10^5 weighted (i.e., by rate $\varpi(t_0)$) classical trajectories of electron pairwise are traced and a few thousands or more of DI events are collected for statistics. Convergency of the numerical results is further tested with increasing the number of launched trajectories twice.

Results and Discussions.— Nitrogen molecule is used to demonstrate our theory. The internuclear separation is 2.079 a.u. and $I_{p1} = 0.5728$ a.u., $I_{p2} = 0.9989$ a.u.. The laser frequency is $\omega = 0.05695$ a.u. corresponding to a wavelength of 800 nm. The number of optical cycle is chosen as 37 a.u. to match the experiments of Cornaggia[3]. The ratio between double and single ionization yield is plotted with respect to the peak laser intensities from 5×10^{13} W/cm² to 1×10^{15} W/cm² in Fig.1.

The threshold value of 0.185 PW/cm² separates the DI data into two parts. When peak laser intensity is below this value, there exist two dominant processes responsible for emitting both electrons, namely, collision-ionization(CI) and collision-excitation-ionization(CEI), as shown in Fig.3(a)(b), respectively. For CI, the tunnelled electron is driven back by the oscillating laser field to collide with the bounded electron near its parent ions causing an instant (\sim attosecond) ionization. For CEI, DI event is created by recollision with electron impact

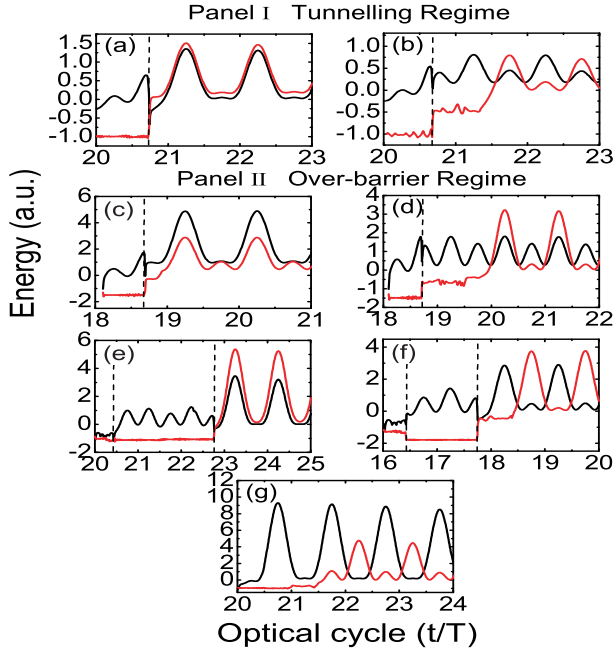


FIG. 3: (color online). Typical energy evolution of the electron pair in both tunnelling regime and over-barrier regime. Vertical dashed lines indicate the moment when collision between electrons emerge.

excitation followed a time-delayed (\sim a few optical periods) field ionization of the excited state. When the instantaneous laser field is above the threshold value, over-barrier ionization emerges. In this regime we observe more complicated trajectories for DI processes. Except for CI (Fig.3(c)) and CEI (Fig.3(d)) trajectories similar to tunnelling case, there are multiple-collision trajectories as shown in Fig.3(e),(f) as well as collisionless trajectory of Fig.3(g). In Fig.3(e) and (f), initially two valence electrons entangle each other, experience a multiple-collision and then emit. The four types of trajectories indicated by Fig.3(c-f) represent the dominant processes of DI in the plateau regime from 0.185 PW/cm^2

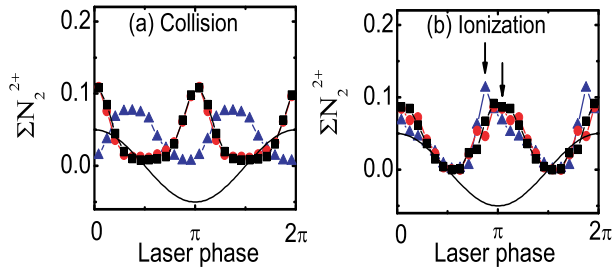


FIG. 4: (color online). DI yield vs laser phase when (a) the two electrons become closest; (b) both the electrons are ionized, at different laser intensity 0.12 PW/cm^2 (triangle), 0.4 PW/cm^2 (circle) and 1 PW/cm^2 (square), respectively.

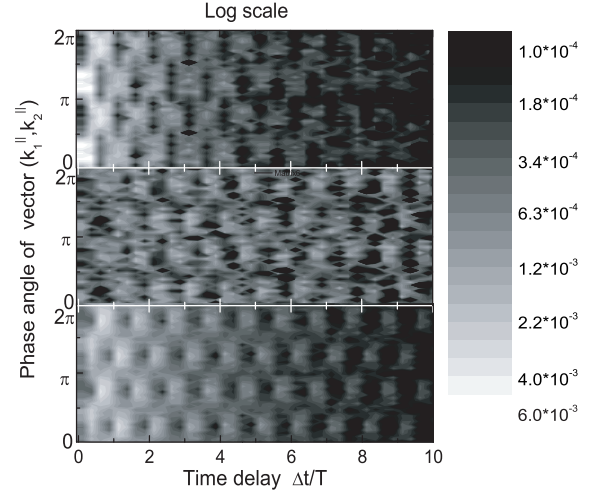


FIG. 5: (color online). The relationship between the correlated momentum and the delay time at (a) 0.12 PW/cm^2 (b) 0.4 PW/cm^2 (c) 1.0 PW/cm^2

to 0.5 PW/cm^2 , that are much more complicated than that of tunnelling regime, but still accompanied by once or multiple times of collisions between two electrons[16]. However, above 0.5 PW/cm^2 , the DI is dominated by a collisionless sequential ionization whose typical trajectory is represented by Fig.3(g). In this regime results from our model agree with ADK theory.

Analysis on trajectories of e-e pairs achieves insight into the complicated dynamics of DI, where important information is indicated by the laser field phase at the moments of collision and ionization[17, 18]. We choose three typical laser intensities, 0.12 PW/cm^2 , 0.4 PW/cm^2 and 1 PW/cm^2 , representing the tunnelling regime, plateau regime and sequential ionization regime, respectively.

Fig.4(a) shows the diagram of DI yield vs laser phase at the moment of closest collision. In the tunnelling regime (i.e., 0.12 PW/cm^2), we note that the collision can occur throughout most of the laser cycle and the peak emerges slightly before the zeroes of the laser field, consistent with the prediction of simple-man model[19] and recent results from purely classical calculation[9]. However, for other two cases, the collision between two correlated electron turns to occur mainly at peak laser field. This is because ionization mechanism changes at the transition to over-barrier regime, where both electrons rotate around nuclei and their distance could be very close before one of them is driven away by the external field.

Fig.4(b) confirms that most DI occurs around the maximum of laser field for both tunnelling regime and over-barrier regime. More interestingly, compared to two other cases we observe a peak shift of $\sim 30^\circ$ off the field maximum for the tunnelling case. It is due to the larger fraction of CI trajectories in this regime. With assuming that the colliding electrons leave the atom with no significant energy and electron-electron

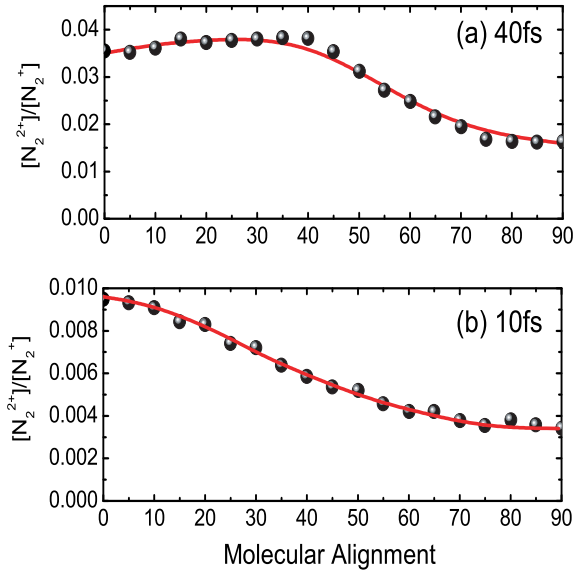


FIG. 6: (color online). The molecular alignment dependence of DI ratios for laser intensity of 0.15 PW/cm^2 . The full circles are our numerical results and the solid lines are guided by eye.

momentum exchange in final state is negligible (these assumptions have been checked by directly tracing trajectories), the parallel momentum $k_{1,2}^{\parallel}$ of each electron results exclusively from the acceleration in the optical field: $k_{1,2}^{\parallel} = \pm 2\sqrt{U_p} \sin \omega t_{ion}$ [18]. The above shifted peak indicates the accumulation of the emitted electrons at $k_1^{\parallel} = k_2^{\parallel} = \pm 0.5 a.u.$ in the first and third quadrants of parallel momentum plane ($k_1^{\parallel}, k_2^{\parallel}$). It is consistent with the experimental data of Ref.[7] (see their Fig.2).

Fig.5 shows the phase angle of momentum vector ($k_1^{\parallel}, k_2^{\parallel}$) with respect to the delayed time between the closest collision and ionization. Integrating over angle gives total DI yield vs the delayed time. In all three cases we observe a long-tail up to several optical periods. For the sequential ionization of 1 PW/cm^2 , it means after one electron is deprived from nuclei by laser fields the other electron is slowly (i.e., waiting for up to 10 optical periods) ionized. In the tunnelling regime, the long-tail indicates that CEI mechanism is very pronounced for the molecular DI (contribute to 80% of total DI yield). This observation is different from purely classical simulation [9], where CI effect is believed to be overestimated. Our results, however, are consistent with experiments of Ar atom [17], where ionization potential and laser field pa-

rameters are close to our case. The reason is stated as follows. For the intensity of 0.12 PW/cm^2 , the maximal kinetic energy of the returned electron is $3.17 U_p = 0.85 a.u.$, still smaller than the ionization energy of N_2^+ . Even with the assistance of the Coulomb focusing [20], it is not easy for the returned electrons to induce too many CI events.

The regular pattern in Fig.5(a),(c) exhibit that the ejection of electrons in the same-hemisphere and opposite-hemisphere emerge alternately with respect to the delayed time. For a time delay of odd half laser cycles, two electrons emit in the same direction, for a time delay of even half laser cycles, two electrons emit in the opposite direction. Moreover, in the tunnelling regime the pattern in Fig.5(a) shows two signally bright spot in the first and third quadrants when the delayed time is less than $0.5T$, a phenomenon directly due to the CI trajectories. The above observation supports the picture of attosecond electron thermalization of tunnelling regime [21]. On the other hand, the irregular pattern emerges in Fig.5(b) for DI in the plateau regime as the signature of complicated multiple-collision trajectories.

In our producing data in Fig.1 the molecular alignment is set to be random and our result is obtained by averaging over different alignment directions. Recent progress in experimental technique makes it possible to control molecular alignment by applying a weak pre-pulse [7]. With this consideration and further application of our model, we calculate the ratios between double and single ionization according to different molecular alignment angles. Main results are presented in Fig.6. It shows that, i) The ratio between DI and single-ionization yield is less for perpendicular molecules than that of parallel molecules; ii) This anisotropy becomes more dramatic for a shorter laser pulse. Further explorations show that molecular alignment also significantly affects the correlated momentum distribution of emitted electrons. Details will be presented elsewhere [12].

In summary, we have developed a semiclassical quasi-static model that can be used to compared with experimental data of molecular DI quantitatively under the relevant experimental conditions, i.e., highly nonperturbative fields with femtosecond or shorter time resolution. With this model, we have achieved insight into the DI dynamics of molecules and revealed the significant effect of molecular alignment on DI yield. The latter can be regarded as our theoretical prediction waiting for test from future's experiments.

This work is supported NNSF of China under Grant No.10574019, and CAEP Foundation 2006Z0202.

[1] Th.Weber *et al.*, Nature (London) 405, 658 (2000).
 [2] C.Guo, M.Li, J.P.Nibarger, and G.N.Gibson Phys. Rev. A 58, R4271 (1998).
 [3] C.Cornaggia and Ph.Hering, Phys. Rev. A **62**, 023403 (2000).

[4] X. Liu, H. Rottke, E. Eremina, W. Sandner, E. Goulielmakis, K. O. Keeffe, M. Lezius, F. Krausz, F. Lindner, M. G. Schätzel, G. G. Paulus, and H. Walther, Phys. Rev. Lett. **93**, 263001 (2004).
 [5] A.S.Alnaser, S.Voss, X.-M.Tong, C.M.Maharjan,

- P.Ranitovic, B.Ulrich, T.Osipov, B.Shan, Z.Chang, and C.L.Cocke, Phys. Rev. Lett. **93**, 113003 (2004)
- [6] E.Eremina, X.Liu, H.Rottke, W.Sandner, M.G.Schätzel, A.Dreischuh, G.G.Paulus, H.Walther, R.Moshammer, and J.Ullrich, Phys. Rev. Lett. **92**, 173001 (2004)
- [7] D. Zeidler, A. Staudte, A.B.Bardon, D.M.Villeneuve, R. Dörner, and P. B. Corkum, Phys. Rev. Lett. **95**, 203003 (2005).
- [8] See, for example, J.S.Parker *et al.*, J. Phys. B **36**, L161 (2004); A Becker and F H M Faisal, J. Phys. B **38** (2005) 1C56
- [9] S.L.Haan, L.Breen, A.Karim, and J.H.Eberly, Phys. Rev. Lett. **97**, 103008 (2006), and references therein.
- [10] Jakub S.Prauzner-Bechcicki, Krzysztof Sacha, Bruno Eckhardt, and Jakub Zakrzewski, Phys. Rev. A **71**, 033407 (2005).
- [11] The atomic ADK theory has been extended to molecule with two-center, see for example, X.M.Tong *et al.*, Phys. Rev. A **66**, 033402 (2002) and Corkum *et al.*, Phys. Rev. Lett. **90**, 233003 (2003) and explicit analytic expression derived in [12]. However, we still exploit the atomic version of ADK formula, i.e., $\varpi(t_0) = \frac{4(2I_{p1})^2}{\varepsilon(t_0)} \exp(-\frac{2(2|I_{p1}|)^{3/2}}{3\varepsilon(t_0)})$. This is done not only for convenience but more importantly because we recognize that in our following calculating the ratios between double ionization and single ionization, this approximation does not leads to significant discrepancy.
- [12] Y.Li, J.Chen, S.P.Yang, and J.Liu, 'Correlated momentum distribution of double-ionized molecules', in preparation.
- [13] R.Abrines and L.C. Percival, Proc.Phys.Soc. London **88**, 861 (1966); J.G. Leopold and I.C. Percival, J.Phys.B **12**, 709 (1979).
- [14] Li-Bin Fu, Jie Liu, Jing Chen, and Shi-Gang Chen Phys. Rev. A **63**, 043416 (2001); J. Chen, J. Liu, L. B. Fu, and W. M. Zheng Phys. Rev. A **63**, 011404 (2001); Li-Bin Fu, Jie Liu, and Shi-Gang Chen Phys. Rev. A **65**, 021406 (2002); J. Chen, J. Liu, and W. M. Zheng Phys. Rev. A **66**, 043410 (2002).
- [15] L.Meng, C.O.Reinhold and R.E.Olson, Phys. Rev. A **40**, 3637 (1989).
- [16] G. G. Paulus, W. Becker, W. Nicklich and H. Walther, J. Phys. B: At. Mol. Opt. Phys. **27** L703-L708 (1994).
- [17] B. Feuerstein, R. Moshammer, D. Fischer, A. Dorn, C. D. Schröter, J. Deipenwisch, J. R. C. Lopez-Urrutia, C. Höhr, P. Neumayer, J. Ullrich, H. Rottke, C. Trump, M. Wittmann, G. Korn, and W. Sandner, Phys. Rev. Lett. **87**, 043003 (2001).
- [18] M.Weckenbrock D. Zeidler, A. Staudte, Th. Weber, M. Schöffler, M. Meckel, S. Kammer, M. Smolarski, O. Jagutzki, V. R. Bhardwaj, D. M. Rayner, D. M. Villeneuve, P. B. Corkum, and R. Dörner, Phys. Rev. Lett. **92**, 213002 (2004).
- [19] P. B. Corkum, Phys. Rev. Lett. **71**, 1994 (1993).
- [20] T.Brabec, M.Yu.Ivanov, and P.B.Corkum, Phys. Rev. A **54**, R2551 (1996).
- [21] X. Liu, C. Figueira de Morisson Faria, W. Becker and P. B. Corkum, J. Phys. B **39**, L305 (2006).